Photochemistry Illuminates Ubiquitous Organic Matter Fluorescence Spectra
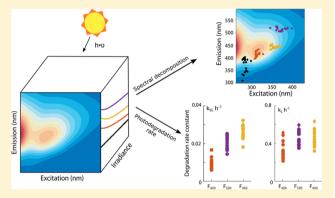
(article starts on next page)

Photochemistry Illuminates Ubiquitous Organic Matter Fluorescence Spectra

K. R. Murphy,*,[†] S. A. Timko,[‡] M. Gonsior,[§] L. C. Powers,[§] U. J. Wünsch,[†] and C. A. Stedmon[∥]

[†]Architecture and Civil Engineering, Chalmers University of Technology, 41296 Gothenburg, Sweden

[‡]Kennedy/Jenks Consultants 1191 Second Avenue, Suite 630 Seattle, Washington 98101, United States

[§]University of Maryland Center for Environmental Science, Chesapeake Biological Laboratory, 146 Williams Street, Solomons, Maryland 20688, United States

[∥]National Institute of Aquatic Resources, Technical University of Denmark, 2800 Kongens Lyngby, Denmark
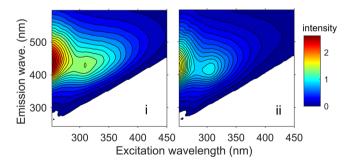
S *Supporting Information*

ABSTRACT: Dissolved organic matter (DOM) in aquatic environments forms a vast reservoir of carbon present as a complex supermixture of compounds. An efficient approach to tracking the production and removal of specific DOM fractions is needed across disciplines, for purposes that range from improving global carbon budgets to optimizing water treatment in engineered systems. Although widely used to study DOM, fluorescence spectroscopy has yet to deliver specific fractions with known spectral properties and predictable distributions. Here, we mathematically isolate four visible-wavelength fluorescent fractions in samples from contrasting lake, river, and ocean environments. Using parallel factor analysis (PARAFAC), we show that most measured fluorescence in environmental samples can be explained by ubiquitous spectra with nearly stable optical properties and photodegradation behaviors over environmental pH gradients. Sample extraction changed bulk fluorescence spectra but not the number or shape of underlying PARAFAC components, while photobleaching preferentially removed the two longest-wavelength components. New approaches to analyzing fluorescence data sets incorporating these findings should improve the interpretation of DOM fluorescence and increase its utility for tracing organic matter biogeochemistry in aquatic systems.

INTRODUCTION

Dissolved organic matter (DOM) composition and concentration varies within and across aquatic systems depending on source and exposure to degradation processes.[1−3] Although only a fraction of DOM contains conjugated π-electron systems that fluoresce,[4] fluorescent DOM (FDOM) frequently tracks the wider DOM pool in the environment.[5] For this reason and due to the relative ease of obtaining sensitive, cost-effective measurements, FDOM is frequently used as a proxy for DOM as a whole.[5−7] Fluorescence excitation emission matrices (EEMs) obtained by scanning across multiple wavelengths (Figure 1) can be assembled into multiway data sets that can be mathematically decomposed using parallel factor (PARAFAC) analysis.[8] PARAFAC assumes that the fluorescence signal is the sum of emission by a limited number of unique, noninteracting components with independent spectral characteristics, and identifies these using an iterative fitting algorithm.[9] When Beers Law is upheld, fluorophores are noninteracting, fluorescence spectra are corrected for optical artifacts, and the correct number of components is assumed, then PARAFAC is capable of revealing the pure chemical

Figure 1. Fluorescence EEM of a riverine DOM extract (i) before and (ii) after 20 h of simulated solar irradiation.

spectra of the major underlying fluorescent moieties in known mixtures, and their concentrations in each sample.[8] In complex mixtures like DOM, the purity of PARAFAC spectra, and

relationships between fluorescence intensity and concentration of the responsible chemical moieties, are both unknown.

Over the past decade, PARAFAC has evolved to become the most widely used statistical tool for characterizing FDOM across a broad range of applications.[9−11] Numerous studies show broadly similar PARAFAC spectra occurring across diverse aquatic environments;[10,12] however, the specific fluorescent components that unambiguously signify discrete DOM fractions have remained elusive. Meanwhile, criticism of the PARAFAC approach has mounted. Spectrally similar components are frequently reported to exhibit contrasting responses to similar physical and chemical gradients.[10] Between data sets[10,12] and among subsets of data,[13,14] PARAFAC components can vary in peak position and spectral shape. Multiple studies report that long-wavelength fluorescence depends upon intramolecular charge-transfer interactions between electron-rich donors (e.g., polyhydroxylated aromatics) and electron-poor, carbonyl-containing acceptors formed from lignin precursors.[15−17] The strength of such interactions would be expected to vary between samples and data sets depending on the sample matrix and electronic environment. Should electronic interactions within or between components significantly change the spectral properties of the underlying fluorescence components between samples, then the underlying data structure would not be trilinear. In that case, PARAFAC assumptions would be violated making the model mathematically and chemically meaningless.[8] Many have therefore concluded that PARAFAC is incapable of retrieving the individual fluorescence spectra of DOM moieties nor delivering significant insights into the molecular structures responsible for fluorescence.[4,17]

A critical prerequisite to successful PARAFAC modeling is a data set encompassing sufficient compositional variability and lacking excessive noise.[8] The number of PARAFAC components identified and validated in DOM data sets increases with sample size,[18] suggesting that larger data sets favor greater sensitivity. At the same time, geographically and chemically diverse data sets often produce unstable PARAFAC models,[13] ostensibly due to high chemical complexity. This tension between large sample sizes to encompass measurable variability and small sample sizes to limit mathematical complexity creates a paradox that has severely hampered further developments in this field. A potential resolution to this paradox is to create multiway data sets from individual DOM samples.[19] We implemented this approach by exposing DOM extracts to simulated solar irradiation under controlled pH in a recirculating flow cell.[20] The induced fluorescence changes allowed us to mathematically isolate independently varying components. Analyzing each extract independently reduced complexity and bias and ensured that environmental gradients other than photodegradation were reduced or eliminated.

■ METHODS

Thirty-five data sets were created and analyzed independently in this study. Each data set was derived from one of 20 samples of aquatic DOM obtained from diverse natural waters, spanning dark-water samples dominated by decomposing terrestrial plant matter, clear-water lakes, and samples originating far from terrestrial sources and having exclusively aquatic DOM (Table S1). Three samples represented filtered (0.2 μm) whole-water samples containing bulk DOM, the remainder were isolates extracted using reverse osmosis (RO), solid-phase extraction (PPL[21]), or XAD resin.

The bulk water samples came from the surface of rivers and lakes in the Amazonian basin. The PPL isolates were from rivers and lakes in Sweden, China, Antarctica, North America and Brazil, or from the North Atlantic open ocean and marginal seas, including a deep-water (4534 m) BATS site in the Sargasso Sea. Commercial Suwannee River standard reference material extracted via reverse osmosis was acquired from the International Humic Substances Society (SRNOM, 2R101N). Antarctic DOM from 9 m depth in Lake Fryxell was isolated on an XAD resin.[22] Molecular analyses using high resolution mass spectrometry indicate that the data set included samples with diverse chemical and molecular compositions.[22,23]

A custom-built irradiation system described previously[20] was used to photodegrade each sample at constant pH in separate experiments. Briefly, samples were continuously pumped at a rate of ∼2.5 mL min^{-1} through the irradiation system via an equilibration vial (allowing for temperature and pH control and to prevent oxygen consumption) to a recirculating flow cell (10 × 4 mm or 3 × 3 mm) located in the spectrofluorometer (Horiba Aqualog). The irradiation system consists of a SCHOTT Borofloat borosilicate glass spiral flow cell (Hellma Analytics, 70−85% transmission between 300 and 350 nm, 85% transmission at wavelengths >350 nm) located underneath an Oriel Sol2A Class ABA solar simulator (Newport Corporation) equipped with a 1000 W xenon arc lamp with an AM 1.5 filter. Lamp power was measured using a Newport 91150 V Reference Cell and adjusted to 1000 W/m^2 with a Newport 68951 Digital Exposure controller. Under these conditions and with this irradiation design, samples received a photon dose of 157 mE m^{-2} h^{-1} (330−380 nm) determined using nitrite actinometry.[24]

Before each experiment, sample absorbances were between 0.05 and 1.0 at 254 nm corresponding to initial DOC values of <1−50 mg L^{-1} (Table S1). Each sample was photodegraded at pH = 8.0 for 20 h. Five aliquots of SRNOM were additionally irradiated in triplicate experiments each at constant pH = 4, 5, 6, 7, and 8 creating 15 additional data sets. Spectral data were collected in batch mode at 20 min intervals; each experiment thus lasted a full day, while the triplicate experiments of SRNOM irradiated at five different pH represent 15 full days of measurements. Each experiment produced a data set containing approximately 60 fluorescence excitation−emission matrices spanning wavelengths from 250 to 600 nm at approximately 3 nm intervals plus matching absorbance spectra. Absorbance spectra were corrected for baseline shifts, fluorescence was corrected for spectral and inner filter effects,[20] and the EEMs from each experiment were assembled into individual three-way (exposure × excitation × emission) data sets.

PARAFAC models were developed independently for each sample using drEEM[14] and the PLS_toolbox (eigenvector Inc.) in MATLAB. Models (4−5 components) were developed with non-negativity constraints on each mode and a convergence criterion of 10^{-10}. Each model was run 50 times after initializing with different randomly generated starting values, and only the least-squares (minimum error) solution was retained. Excitation wavelengths below ∼270 nm with disproportionately high influence on the model were removed. The final four-component models accounted for >99.9% of the measured spectral variation in each data set.

In traditional PARAFAC modeling of multisample data sets, validation is performed by splitting a data set into independent

halves, modeling each half separately, then comparing the results. If the models for each half are sufficiently similar then the model is considered validated and the EEM data set is replaced by the PARAFAC spectra and scores.[9] In the present case, splitting data sets in two would have been meaningless because the halves would be dependent (from the same sample). Instead, the validation test was to compare each model with every other model in the data set, regardless of sample age, origin or pretreatment. This is the strongest validation ever attempted for DOM-PARAFAC data sets.

PARAFAC scores are proportional to fluorescence intensity and photodegradation rate constants were determined by separately fitting a double exponential function to the PARAFAC scores for each component in each sample.[20] Fluorescence (f) at time t was modeled as the loss of the photolabile (L) and semiphotolabile (SL) fractions at rate constants k:

$$f_t = f_L e^{-k_L t} + f_{SL} e^{-k_{SL} t}$$

Rate constants were determined only where f_t adhered closely to a double exponential function, and thus were undetermined for the Cape Evans sample and for F_{420} in the Lake Erhai sample. Fluorescence indices (FI, BIX) were calculated for each sample at the beginning and end of irradiation experiments. FI, also known as the fluorescence index,[25] was calculated from the ratio of the fluorescence emission at 470 to 520 nm at 370 nm excitation.[26] The freshness index[27] (BIX) was calculated as the ratio of emission at 380 nm to the maximum emission within the range of 420–435 nm following excitation at 310 nm.[28] Traditionally, FI is used to distinguish DOM source with low ratios (~1.2) representing terrestrial end-members and high ratios (~1.8) representing microbial end members. BIX is used as a proxy of DOM age, with higher ratios indicating a preponderance of recently created DOM from microbial sources over older, more recalcitrant DOM.

■ RESULTS AND DISCUSSION

Figure 2 shows each component in each sample mapped according to its excitation peak (corresponding to the lowest-energy absorbance band) and fluorescence emission peak position. The Stokes shift, representing the energy difference between these positions, varied between 0.42 and 1.35 eV, thus falling within the same range that is observed for pure organic compounds.[29] Reoccurring PARAFAC components appeared in all models at 397 ± 7 nm, 417 ± 10 nm, 445 ± 6 nm, and 514 ± 9 nm. These were named F_{400}, F_{420}, F_{450}, and F_{520}, corresponding to the median positions of emission maxima (397, 416, 446, and 516 nm, respectively).

Between data sets, the derived components were highly spectrally similar whether comparing (i) PPL extracts with their matching bulk samples (Figure 3A; SI S2); (ii) RO extracts degraded at different pH (Figure 3B); (iii) various rivers and lakes (Figure 3C); or (iv) terrestrial river/lake versus autochthonous deep-sea/Antarctic samples (Figure 4A). The ubiquitous spectra were also highly congruent with one-sample HPSEC-EEM-PARAFAC spectra[19] (Figure 4C) although HPSEC separates components by size instead of photochemical reactivity. Whereas DOM extraction preserved fluorescence spectral shapes, extraction efficiencies varied between components, with PPL samples containing relatively
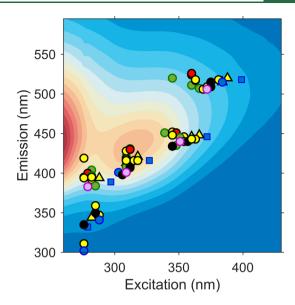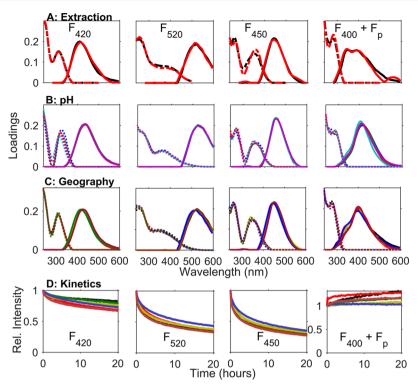

Figure 2. Positions of fluorescence peak maxima in allochthonous and autochthonous DOM. Each point was obtained from the PARAFAC decomposition of a single sample at pH = 8. Samples were bulk DOM (triangles) or extracts (PPL: circles, RO: diamonds, XAD: squares) sourced from Suwannee River (red), rivers and lakes in South America (yellow), Swedish rivers and lakes (green), a Chinese lake (mauve), Antarctica (blue) or the North Atlantic (black). Contour plot in background depicts fluorescence of a standard reference material (SRNOM).

less F_{420} and relatively more F_{450} than their corresponding bulk samples (SI S2).

In contrast to the other components, F_{400} emission spectra varied strongly between samples due to an emission shoulder of variable height located near 340 nm. This indicated that F_{400} must represent two or more components having similar excitation spectra but different extraction efficiencies. This conclusion was supported by (a) a fifth component (F_p) with a broad, indistinct emission and a variably sized protein-like peak, observed in five-component PARAFAC models of several samples, e.g. from the Sargasso and Antarctica (Figure 4A, B), and (b) the absence of a shoulder on a similar component in RO extracts and size-fractionated EEMs (Figure 4C).

Despite the extreme diversity in sample origin and pretreatment, photodegradation of each component followed similar kinetics in each sample (Figure 3D, SI S3) even when varying pH (SI S4). In four-component models, component F_{400} was stable under irradiation or slightly increased. Feasible five-component models were obtained for a subset of samples, whereby F_{400} resolved into two separate components (F_{400} + F_p), while other spectra were practically unchanged relative to a four-component model. In five-component models, F_{400} was removed slowly (<10% over 20 h) according to pseudo-first-order degradation kinetics and F_p alone was produced (SI S3). The slow decay by component F_{400} can be explained by the poor overlap between its excitation spectrum (F_{400} primarily absorbs below 300 nm) and the spectral output of the solar lamp (lamp emits above 300 nm), that is, F_{400} is not necessarily photorefractory.

For the three photolabile components, decay kinetics were characterized by initially fast followed by slower rates of photodegradation. When fitted to a double exponential function,[20] the photolabile (fast) rate constants (k_L) decreased in the order: $F_{450} \gtrsim F_{520} > F_{420}$. In contrast, the semilabile

Figure 3. Fluorescence spectra and intensities extracted from independent PARAFAC models of DOM changing under photodegradation. Panel A: A bulk sample (red) compared to a PPL extract (black), both from Pantanal Lake 3 and photodegraded at pH 8. Excitation spectra appear to the right of emission spectra. Panel B: Commercial SRNOM, extracted by reverse-osmosis and photodegraded at pH 4, 5, 6, 7, and 8. Panel C: PPL-extracted DOM from six lakes and rivers in Sweden and the Americas, photodegraded at pH 8. Panel D: Relative fluorescence intensities showing reaction kinetics for the six PPL extracts in panel C.
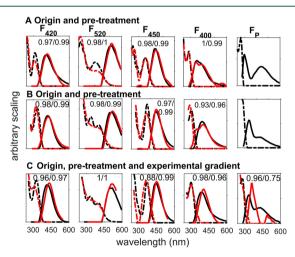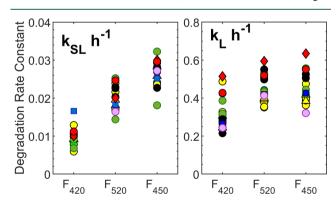

Figure 4. Comparisons between fluorescence spectra in data sets with different DOM origin (allochthonous vs autochthonous), pretreatment (bulk water, PPL extract, XAD extract) and experimental gradients (photodegradation vs HPSEC). In each plot, Tucker congruence is shown between matched pairs of excitation and emission spectra (rex/rem). Panel A: Amazon Pantanal Lake 3 (red, whole-water, 4-component model) compared to the Sargasso Sea at 4534 m depth (black, PPL extract, 5-component model). Panel B: Amazonian Rio Negro (red, whole-water, 4-component model) compared to Antarctic Lake Fryxell, (black, XAD extract, 5-component model). Panel C: HPSEC model for Rio Tapajos[29] (red, PPL extract, 5-component model) compared to photochemistry model for Antarctic Lake Fryxell (black, XAD extract, 5-component model).

(slow) photodegradation rate constants (k_{SL}) differed systematically between components and for a single component, were consistent across the data set regardless of sample source or pretreatment (Figure 5). Across the data set at pH = 8, k_{SL} (h^{-1}) for F_{420}, F_{520}, and F_{450}, was 0.010 ± 0.0017 ($N = 16$), 0.021 ± 0.0033 ($N = 18$), and 0.027 ± 0.0033 ($N = 18$). These rates are each significantly different ($p < 0.0001$) according to repeated-measures ANOVA with pairwise comparisons of means. Coefficients of variation (CV = std. dev./mean) ranged

Figure 5. Semilabile (k_{SL}) and labile (k_L) degradation rate constants for ubiquitous fluorescence components in diverse water samples. Each data point represents the rate constant determined at pH = 8 from the PARAFAC decomposition of a single sample. Plots show bulk DOM (triangles) and extracts (PPL, circles; RO, diamonds; XAD, squares). Samples were sourced from Suwannee River (red), rivers and lakes in South America (yellow), Swedish rivers and lakes (green), an Antarctic lake (blue), a Chinese lake (mauve), or the North Atlantic (black).

from 12−18%, excluding only F_{420} in the lake Fryxell sample. The level of variation in k_{SL} across the data sets is therefore similar to the variation that was observed between replicate experiments involving a single sample of standard SRNOM photodegraded at pH = 8 (CV = 18−33%, SI S4). Since fluorescence measurement error is typically small and double-exponential models almost always provided excellent fits ($R^2 >$ 0.99), much of the observed variability must have arisen from experimental error, that is, a combination of irradiation and PARAFAC-modeling error.

The double-exponential decay kinetics of PARAFAC components suggest that photodecomposition occurred by more than one pathway. In addition to causing direct photobleaching of chromophores, absorption of light by organic chemicals produces a range of photochemically produced reactive species involved in indirect photodegradation of DOM, including triplet excited states ($^3DOM^*$) which both oxidize organic compounds and react with other species to produce further oxidants.[30] Since the labile rate constants appeared to reflect a property of samples that was shared between PARAFAC components, this implies an important role of the sample matrix in determining k_L, potentially via different relative concentrations of $^3DOM^*$ precursors[31] and different $^3DOM^*$ compositions and reactivities.[30,32] Across the dataset, a weak positive correlation ($R^2 = 0.22$, F = 4.1, df = 15, p = 0.06) between DOC and average k_L provides potential support for a link between labile decay rates and DOM concentration. In contrast, the semilabile rate constants were independent of sample matrices and may therefore represent direct photodegradation rates for the respective components under simulated solar irradiation. Further experiments are warranted to test these hypotheses and establish the interpretation of the decay rates with greater certainty.
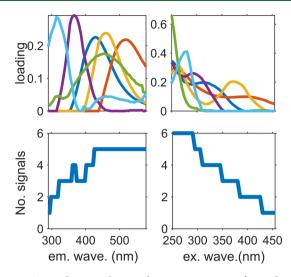
The observed high statistical congruence between fluorescence spectra and decay behaviors in different samples despite variable DOM composition, and varying chemical and analytical interferences, provides strong evidence that the data conformed to a trilinear structure for which the PARAFAC decomposition model was appropriate. The structural origin of the ubiquitous spectra is unknown, but it is likely that there is a pool of organic compounds or fluorophores with nearly identical spectral properties and photochemical behaviors. Time-resolved fluorescence measurements indicate that steady-state measurements tend to be dominated by relatively long-lived fluorophores with high quantum efficiencies;[16,33] thus, it is also possible that the ubiquitous spectra arise from specific fluorophores that are very widely distributed and tend to dominate observed steady-state fluorescence across environmental systems due to long lifetimes and efficient fluorescence. This also offers a simple explanation of the data[34] and if true, it seems likely that relatively simple molecular structures at the end of the biogeochemical degradation continuum must be responsible. However, resolving these questions is impossible at present due to the absence of instruments and methods capable of isolating fluorescent from nonfluorescent DOM at the same time as determining both molecular formulas and molecular structures. Although ultrahigh-resolution mass spectrometry (HRMS) identifies exact masses and their molecular formulas in DOM,[35] it does not routinely recover the structural data needed to confirm the presence of aromatic rings. Furthermore, HRMS recoveries vary for different molecules due to variable ionization efficiencies, introducing artifacts and high risk of false positive/negatives if attempting to correlate molecular formula tables with fluorescence intensities to identify the responsible fluorescent molecules.[5]

Fluorescence components similar to F_{420}, F_{450}, F_{520}, and F_P have been widely observed in DOM-PARAFAC models from diverse aquatic environments, but quantitative evaluations of spectral similarity across systems are lacking. The widespread occurrence of statistically similar spectra in published literature was confirmed using the OpenFluor database,[12] which compares fluorescence data sets and determines Tucker congruence (r) between pairs of excitation (r_{ex}) and emission (r_{em}) spectra. Published data sets containing very strong matches for all three of F_{420}, F_{450}, and F_{520}, include PARAFAC models of fluorescence spectra from the Danish Kattegat,[36] San Francisco Bay,[14] and Shark Bay[37] in Australia. Overall, compared to 73 published data sets currently in OpenFluor, the percentage containing a strong match ($r_{ex} \times r_{em} > 0.95$) for F_{420}, F_{450}, and F_{520} was approximately 30%, 15%, and 20% respectively. These are relatively high match rates considering the many potential sources of differences between published studies, including different instrument optics, sample types, methods and experimental conditions. Components F_{520} and F_{420} (SI S5) were especially highly congruent between samples in this study, as well as with published FDOM-PARAFAC and HPSEC-PARAFAC spectra (SI S6).

New insights affecting the practical application of PARAFAC were obtained from data analyses. Approximately 70% of data sets in OpenFluor did not contain strong matches for F_{450} or F_{520}, but instead featured a single long-wavelength peak with intermediate properties. We suspect this is because F_{450} and F_{520} have rather similar photodegradation rates (Figure 5), causing the two signals to be highly correlated in data sets influenced by sunlight. Since models with highly correlated component intensities will have low PARAFAC core-consistencies,[38] using the core-consistency criterion as a model diagnostic is likely to routinely produce models that are under-specified. Furthermore, in most statistical comparisons between pairs of samples, congruence between emission spectra was systematically higher than between excitation spectra (SI S5). This is also evident from emission peak positions, which cluster tightly across the data set in contrast to excitation peak positions (Figure 2). While the diversity in excitation spectra may reflect a range of factors including greater susceptibility to matrix effects, as suggested by experiments at varying pH (SI S4), it may also result from other artifacts as discussed below.

While samples in this study were dominated by humic-like signals and four components explained nearly all measured fluorescence variation, additional components certainly exist and for specific samples or in specific environments, could explain a substantial proportion of measured signals. Although careful wavelength selection enabled the PARAFAC decomposition of most data sets we tested, surface ocean samples typically failed to produce stable models, presumably due to a fatal combination of previous exposure to sunlight, low initial fluorescence intensities and dominant UV-A fluorescence. UV-A fluorescence signals ($Ex_{max} < 300$ nm, $Em_{max} < 400$ nm, "protein-like") are common in biologically productive environments but in this study were usually indistinguishable from F_{400} since neither absorbed solar irradiation to a significant extent. Abundant UV-A signals could present a significant challenge for PARAFAC by increasing mathematical complexity at wavelengths where spectra are short and steep but data are relatively few (Figure 6) and affected by Rayleigh and Raman

Figure 6. Mathematical complexity, in terms of number of overlapping FDOM spectra, as a function of excitation (ex.) and emission (em.) wavelength (wave.) for a six-component PARAFAC model.[14]

scatter.[8] Additionally, short excitation wavelengths have a disproportionate influence on models due to high absorbances combined with low measurement precision, producing high statistical leverages. Should it be possible to presume the spectral properties of some DOM components under a ubiquity hypothesis, this would create new opportunities for interpreting challenging samples containing many overlapping signals. For example, the Pantanal Lake 12 bulk sample had a prominent peak at 340 nm and produced no distinct PARAFAC solution if varying the excitation wavelength range (SI S7). However, the Pantanal Lake 12 data set could be decomposed using the model from Pantanal Lake 3, which is located approximately 80 km away. When the spectra for three "ubiquitous" Lake 3 components were presumed to be present in Lake 12 and PARAFAC was instructed to calculated two further components, this recovered the spectra for the missing "ubiquitous" Lake 3 component plus a feasible UV-A component.

These results have important implications for interpreting DOM fluorescence in aquatic samples. Although visible wavelength (humic-like) DOM fluorescence peaks are still routinely ascribed to "terrestrial" sources, a significant body of research indicates that visible wavelength fluorescence is also produced in the absence of terrestrial sources or humification processes.[39,40] Our results extend this with a demonstration that terrestrially- and autochthonously derived visible fluorescence spectra can be statistically indistinguishable and exhibit identical photodegradation rate constants. In all samples regardless of origin or preparation method, components emitting at long emission wavelengths were photodegraded fastest, explaining why DOM fluorescence invariably shifts toward increasingly shorter emission wavelengths upon photoirradiation.[15,41] Over time, this erodes compositional differences between samples that might once have been attributable to source or biogeochemical processing. In open systems containing spatially variable DOM inputs, the faster photodegradation of F_{450} and F_{520} might easily be misconstrued as biological production of F_{400} and F_{420}. For samples in the current data set, exposure to 20 h artificial solar irradiation caused contradictory changes in commonly reported fluorescence indices (SI S8). The fluorescence index, FI, decreased by up to 20% indicating that irradiated samples appeared increasingly like "terrestrial" DOM, while the freshness index, BIX, increased by up to 37% indicating that samples became more "autochthonous" in character.[26]

Fluorescence spectroscopy is very widely used in studies of DOM biochemistry, and PARAFAC is often used during data interpretation.[28] Many previous studies reported that for various data subsets, PARAFAC components in different samples responded differently to various environmental gradients,[10] often explaining this by differences in DOM source. While this may occur, it is often overlooked that due to PARAFAC trilinearity, systematic biases in model fits are accompanied by systematic biases in model scores. The corollary to this is that if a model does not represent all samples equally well, scores will be affected creating the appearance of systematic differences even when none are present. This is especially likely when representing diverse groups of samples with a single PARAFAC model. However, despite limitations with traditional multisample PARAFAC approaches, it should be remembered that all data interpretation approaches that fail to reliably separate over-lapping fluorescence signals will suffer from similar short-comings.

This study shows that PARAFAC components in DOM EEMs appear to be highly conserved across diverse samples and some of these components respond to environmental stresses (e.g., photobleaching) in predictable ways. Further studies of individual samples subject to controlled environmental gradients are needed both to validate and refine these results, leading to improved interpretations of DOM fate and transformation as assessed by fluorescence spectroscopy. Carefully controlled experiments are also needed to delineate relevant chemical variation attributable to, for example, precursor material and biogeochemical processing, from methodological decisions, such as sample pretreatment or experimental (measurement and modeling) error. Finally, future efforts should determine how best to integrate accumulated knowledge of ubiquitous spectra into data analyses. For example, should certain components be truly ubiquitous, then their presence might be assumed allowing their signals to be subtracted. This could improve the mathematical decomposition of complex samples and may reveal low-abundance fluorescence tracers that are presently impossible to isolate using traditional approaches, including photochemically and microbially labile components not captured in this study.

■ ASSOCIATED CONTENT

Ⓢ Supporting Information

The Supporting Information is available free of charge on the ACS Publications website at DOI: 10.1021/acs.est.8b02648.

> Experimental design, effects of sample extraction, photodegradation kinetics, effects of pH and experimental error on photodegradation rate constants, comparisons with HP-SEC PARAFAC spectra, a novel modeling approach, and photodegradation effects on fluorescence indices and absorbance (PDF)

■ AUTHOR INFORMATION

Corresponding Author
*E-mail: murphyk@chalmers.se. Tel: +46(0)31 772 1936.

ORCID ◉

K. R. Murphy: 0000-0001-5715-3604
U. J. Wünsch: 0000-0001-6972-6932

Notes

The authors declare no competing financial interest.

■ DEDICATION

This paper is dedicated to George Aiken, who generously donated the lake Fryxell extract and was a source of inspiration.

■ REFERENCES

(1) Hansell, D. A. Recalcitrant Dissolved Organic Carbon Fractions. *Ann. Rev. Mar Sci.* **2013**, *5* (1), 421−445.

(2) Nelson, C. E.; Wear, E. K. Microbial diversity and the lability of dissolved organic carbon. *Proc. Natl. Acad. Sci. U. S. A.* **2014**, *111* (20), 7166.

(3) Moran, M. A.; Zepp, R. G. Role of photoreactions in the formation of biologically labile compounds from dissolved organic matter. *Limnol. Oceanogr.* **1997**, *42* (6), 1307−1316.

(4) Aiken, G. R., Fluorescence and Dissolved Organic Matter: A Chemist's Perspective. In *Aquatic Organic Matter Fluorescence*; Coble, P., Baker, A., Lead, J., Reynolds, D., Spencer, R., Eds.; Cambridge University Press: New York, 2014; pp 35−74.

(5) Stubbins, A.; Lapierre, J. F.; Berggren, M.; Prairie, Y. T.; Dittmar, T.; del Giorgio, P. A. What's in an EEM? Molecular Signatures Associated with Dissolved Organic Fluorescence in Boreal Canada. *Environ. Sci. Technol.* **2014**, *48* (18), 10598−10606.

(6) Coble, P. G.; Green, S. A.; Blough, N. V.; Gagosian, R. B. Characterization of dissolved organic matter in the Black Sea by fluorescence spectroscopy. *Nature* **1990**, *348*, 432−435.

(7) Kellerman, A. M.; Kothawala, D. N.; Dittmar, T.; Tranvik, L. J. Persistence of dissolved organic matter in lakes related to its molecular characteristics. *Nat. Geosci.* **2015**, *8* (6), 454−457.

(8) Bro, R. PARAFAC: Tutorial and applications. *Chemom. Intell. Lab. Syst.* **1997**, *38*, 149−171.

(9) Stedmon, C. A.; Markager, S.; Bro, R. Tracing dissolved organic matter in aquatic environments using a new approach to fluorescence spectroscopy. *Mar. Chem.* **2003**, *82*, 239−254.

(10) Ishii, S. K. L.; Boyer, T. H. Behavior of reoccurring PARAFAC components in fluorescent dissolved organic matter in natural and engineered systems: A critical review. *Environ. Sci. Technol.* **2012**, *46* (4), 2006−17.

(11) Moran, M. A.; Kujawinski, E. B.; Stubbins, A.; Fatland, R.; Aluwihare, L. I.; Buchan, A.; Crump, B. C.; Dorrestein, P. C.; Dyhrman, S. T.; Hess, N. J.; Howe, B.; Longnecker, K.; Medeiros, P. M.; Niggemann, J.; Obernosterer, I.; Repeta, D. J.; Waldbauer, J. R. Deciphering ocean carbon in a changing world. *Proc. Natl. Acad. Sci. U. S. A.* **2016**, *113* (12), 3143−3151.

(12) Murphy, K. R.; Stedmon, C. A.; Wenig, P.; Bro, R. OpenFluor-an online spectral library of auto-fluorescence by organic compounds in the environment. *Anal. Methods* **2014**, *6* (3), 658−661.

(13) Murphy, K. R.; Hambly, A.; Singh, S.; Henderson, R. K.; Baker, A.; Stuetz, R.; Khan, S. J. Organic matter fluorescence in municipal water recycling schemes: toward a unified PARAFAC model. *Environ. Sci. Technol.* **2011**, *45* (7), 2909−2916.

(14) Murphy, K. R.; Stedmon, C. A.; Graeber, D.; Bro, R. Fluorescence spectroscopy and multi-way techniques. PARAFAC. *Anal. Methods* **2013**, *5* (23), 6557−6566.

(15) Del Vecchio, R.; Blough, N. V. Photobleaching of chromophoric dissolved organic matter in natural waters: kinetics and modeling. *Mar. Chem.* **2002**, *78*, 231−253.

(16) Boyle, E. S.; Guerriero, N.; Thiallet, A.; Del Vecchio, R.; Blough, N. V. Optical properties of humic substances and CDOM: Relation to structure. *Environ. Sci. Technol.* **2009**, *43* (7), 2262−2268.

(17) Sharpless, C. M.; Blough, N. V. The importance of charge-transfer interactions in determining chromophoric dissolved organic matter (CDOM) optical and photochemical properties. *Environ. Sci. Process Impacts* **2014**, *16* (4), 654−71.

(18) Murphy, K. R.; Bro, R.; Stedmon, C. A., Chemometric analysis of organic matter fluorescence. In *Aquatic Organic Matter Fluorescence*; Coble, P., Baker, A., Lead, J., Reynolds, D., Spencer, R., Eds.; Cambridge University Press: New York, 2014; pp 339−376.

(19) Wünsch, U. J.; Murphy, K. R.; Stedmon, C. A. The one-sample PARAFAC approach reveals molecular size distributions of fluorescent components in dissolved organic matter. *Environ. Sci. Technol.* **2017**, *51* (20), 11900−11908.

(20) Timko, S. A.; Gonsior, M.; Cooper, W. J. Influence of pH on fluorescent dissolved organic matter photo-degradation. *Water Res.* **2015**, *85*, 266−274.

(21) Dittmar, T.; Koch, B.; Hertkorn, N.; Kattner, G. A simple and efficient method for the solid-phase extraction of dissolved organic matter (SPE-DOM) from seawater. *Limnol. Oceanogr.: Methods* **2008**, *6* (6), 230−235.

(22) Aiken, G.; McKnight, D.; Harnish, R.; Wershaw, R. Geochemistry of aquatic humic substances in the Lake Fryxell Basin, Antarctica. *Biogeochemistry* **1996**, *34* (3), 157−188.

(23) Gonsior, M.; Valle, J.; Schmitt-Kopplin, P.; Hertkorn, N.; Bastviken, D.; Luek, J.; Harir, M.; Bastos, W.; Enrich-Prast, A. Chemodiversity of dissolved organic matter in the Amazon Basin. *Biogeosciences* **2016**, *13* (14), 4279−4290.

(24) Jankowski, J. J.; Kieber, D. J.; Mopper, K. Nitrate and Nitrite Ultraviolet Actinometers. *Photochem. Photobiol.* **1999**, *70* (3), 319−328.

(25) McKnight, D. M.; Boyer, E. W.; Westerhoff, P. K.; Doran, P. T.; Kulbe, T.; Andersen, D. T. Spectrofluorometric characterization of dissolved organic matter for indication of precursor organic material and aromaticity. *Limnol. Oceanogr.* **2001**, *46* (1), 38−48.

(26) Gabor, R. S.; Baker, A.; McKnight, D. M.; Miller, M. P. Fluorescence Indices and Their Interpretation. In *Aquatic Organic Matter Fluorescence*; Baker, A., Reynolds, D. M., Lead, J., Coble, P. G., Spencer, R. G. M., Eds.; Cambridge University Press: Cambridge, 2014; pp 303−338.

(27) Parlanti, E.; Wörz, K.; Geoffroy, L.; Lamotte, M. Dissolved organic matter fluorescence spectroscopy as a tool to estimate biological activity in a coastal zone submitted to anthropogenic inputs. *Org. Geochem.* **2000**, *31* (12), 1765−1781.

(28) Zsolnay, A.; Baigar, E.; Jimenez, M.; Steinweg, B.; Saccomandi, F. Differentiating with fluorescence spectroscopy the sources of dissolved organic matter in soils subjected to drying. *Chemosphere* **1999**, *38* (1), 45−50.

(29) Wünsch, U. J.; Murphy, K. R.; Stedmon, C. A. Fluorescence quantum yields of natural organic matter and organic compounds: Implications for the fluorescence-based interpretation of organic matter composition. *Front. Mar. Sci.* **2015**, DOI: 10.3389/fmars.2015.00098.

(30) McNeill, K.; Canonica, S. Triplet state dissolved organic matter in aquatic photochemistry: reaction mechanisms, substrate scope, and photophysical properties. *Environmental Science: Processes & Impacts* **2016**, *18* (11), 1381−1399.

(31) Leresche, F.; von Gunten, U.; Canonica, S. Probing the Photosensitizing and Inhibitory Effects of Dissolved Organic Matter by Using N,N-dimethyl-4-cyanoaniline (DMABN). *Environ. Sci. Technol.* **2016**, *50* (20), 10997−11007.

(32) Boreen, A. L.; Edhlund, B. L.; Cotner, J. B.; McNeill, K. Indirect Photodegradation of Dissolved Free Amino Acids: The Contribution of Singlet Oxygen and the Differential Reactivity of DOM from Various Sources. *Environ. Sci. Technol.* **2008**, *42* (15), 5492−5498.

(33) Clark, C. D.; Jimenez-Morais, J.; Jones, Ii G.; Zanardi-Lamardo, E.; Moore, C. A.; Zika, R. G. A time-resolved fluorescence study of dissolved organic matter in a riverine to marine transition zone. *Mar. Chem.* **2002**, *78* (2−3), 121−135.

(34) McKay, G.; Korak, J. A.; Rosario-Ortiz, F. L. Temperature Dependence of Dissolved Organic Matter Fluorescence. *Environ. Sci. Technol.* **2018**, *52* (16), 9022−9032.

(35) Stenson, A. C.; Marshall, A. G.; Cooper, W. T. Exact Masses and Chemical Formulas of Individual Suwannee River Fulvic Acids from Ultrahigh Resolution Electrospray Ionization Fourier Transform Ion Cyclotron Resonance Mass Spectra. *Anal. Chem.* **2003**, *75* (6), 1275−1284.

(36) Osburn, C. L.; Stedmon, C. A. Linking the chemical and optical properties of dissolved organic matter in the Baltic-North Sea transition zone to differentiate three allochthonous inputs. *Mar. Chem.* **2011**, *126* (1−4), 281−294.

(37) Cawley, K. M.; Ding, Y.; Fourqurean, J.; Jaffé, R. Characterising the sources and fate of dissolved organic matter in Shark Bay, Australia: a preliminary study using optical properties and stable carbon isotopes. *Mar. Freshwater Res.* **2012**, *63* (11), 1098−1107.

(38) Bro, R.; Kiers, H. A. L. A new efficient method for determining the number of components in PARAFAC models. *J. Chemom.* **2003**, *17* (5), 274−286.

(39) Stedmon, C. A.; Nelson, N. The optical properties of DOM in the ocean. In *Biogeochemistry of Marine Dissolved Organic Matter*, 2nd ed.; Hansell, D. A., Carlson, C. A., Eds.; Elsevier: Eastbourne, UK, 2015; pp 481−508.

(40) Jørgensen, L.; Stedmon, C. A.; Granskog, M. A.; Middelboe, M. Tracing the long-term microbial production of recalcitrant fluorescent dissolved organic matter in seawater. *Geophys. Res. Lett.* **2014**, *41* (7), 2481−2488.

(41) Helms, J. R.; Stubbins, A.; Perdue, E. M.; Green, N. W.; Chen, H.; Mopper, K. Photochemical bleaching of oceanic dissolved organic matter and its effect on absorption spectral slope and fluorescence. *Mar. Chem.* **2013**, *155*, 81−91.